

# SCA2003-18: PREDICTION OF OPTIMUM OPERATING CONDITIONS FOR STEADY-STATE TWO-PHASE FLOW IN PORE NETWORK SYSTEMS USING THE *DeProF* TRUE-TO-MECHANISM THEORETICAL MODEL

M.S. Valavanides (1) and A.C. Payatakes (1,2)

(1) FORTH/ICE-HT, (2) Department of Chemical Engineering, University of Patras  
[marval@iceht.forth.gr](mailto:marval@iceht.forth.gr), [acp@iceht.forth.gr](mailto:acp@iceht.forth.gr), Tel. +3061 965301, Fax: +3061 990328

*This paper was prepared for presentation at the International Symposium of the Society of Core Analysts held in Pau, France, 21-24 September 2003*

## ABSTRACT

The recently developed predictive model “DeProF” (acronym for “Decomposition into Prototype Flows”) considers steady-state two-phase flow in porous media as an in-parallel combination of three flow patterns, namely Connected-oil Pathway Flow, Ganglion Dynamics and Drop Traffic Flow. The key difference between these prototype flow patterns is the degree of disconnection of the non-wetting phase ('oil') which, in turn, affects the relative magnitude of the rate of energy dissipation caused by capillary effects compared to that caused by viscous stresses. The observed flow is usually a mixture of the basic prototype flows. Each flow pattern prevails over mesoscopic-scale regions of the porous medium (ranging from a few to several hundred pores), whereas the macroscopic flow is homogeneous.

The predictive capability of the DeProF model was used to investigate whether optimum operating conditions appear in steady-state two-phase flow in pore networks. A new macroscopic dependent variable is determined, namely the *energy utilization factor*. This variable is defined as the ratio of the reduced o/w flow rate ratio over the reduced mechanical energy dissipated; it represents a measure of the efficacy of the physical process in terms of oil transport.

Using DeProF, simulations were carried out over the domain of capillary number,  $Ca$ , and oil-water flowrate ratio,  $r$ , in which two-phase flow is sustainable and for three systems of oil/water/pore network. The results show that, for every system, there exist a continuous line (locus) in the  $(Ca, r)$  domain on which the energy utilization factor attains a local maximum.

## INTRODUCTION

Two-phase flow in porous media (2fFPM) occupies a central position in such physically important processes as enhanced oil recovery, the behavior of liquid organic pollutants near the source in contaminated soils, etc. It has been experimentally observed [1,2] that during two-phase flow the disconnected oil contributes significantly (and in certain cases of practical interest even exclusively) to the flow. Furthermore, the flowrate vs pressure

gradient relation is found to be strongly non-linear, and to be strongly affected by the physical parameters that pertain to the fluid-fluid interfaces.

A recently developed theoretical model [3,4,5,6], predicts the relative permeabilities using the concept of Decomposition in Prototype Flows (DeProF); it accounts for the pore-scale mechanisms and the network wide cooperative effects, and is sufficiently simple and fast for practical purposes. The sources of non-linearity (which are caused by the motion of interfaces) and other complex effects are modeled satisfactorily. The quantitative and qualitative agreement between existing sets of data and the corresponding theoretical predictions of the DeProF model is excellent [5,6].

In the DeProF model it is assumed that in the most general case the macroscopic flow can be decomposed into the two prototype flows, Connected-oil Pathway Flow (CPF) and Disconnected Oil Flow (DOF). The latter comprises Ganglion Dynamics (GD) and Drop Traffic Flow (DTF), regimes which have been observed experimentally [1,2]. Each prototype flow has the essential characteristics of the corresponding flow patterns in suitably idealized form, and so the pore scale mechanisms are incorporated in the prototype flows. The cooperative effects among ganglia and drops are also incorporated in DOF, by making suitable use of a modified version of the effective medium theory [7].

Using the DeProF model, one can obtain the solution to the problem of steady-state two-phase flow in porous media (SS2fFPM) in the form of the following transfer function

$$x = x(\text{Ca}, r; \kappa, \theta_A^0, \theta_R^0, \mathbf{x}_{\text{pm}}) \quad (1)$$

where,  $x = (-\partial\tilde{p}/\partial\tilde{z})\tilde{k}(\tilde{\gamma}_{\text{ow}}\text{Ca})^{-1}$  is the reduced macroscopic pressure gradient,  $\tilde{k}$  is the absolute permeability of the porous medium,  $\text{Ca}$  is the capillary number (defined as  $\text{Ca} = \tilde{\mu}_w \tilde{U}^w / \gamma_{\text{ow}}$ ;  $\tilde{\mu}_w$  is the viscosity of water,  $\tilde{U}^w$  is the superficial velocity of water, and  $\gamma_{\text{ow}}$  is the interfacial tension),  $r = \tilde{q}^o / \tilde{q}^w$  is the oil/water flowrate ratio,  $\gamma = \tilde{\mu}_o / \tilde{\mu}_w$  is the oil/water viscosity ratio,  $\theta_A^0$  and  $\theta_R^0$  are the advancing and receding contact angles and  $\mathbf{x}_{\text{pm}}$  is a parameter vector composed of all the dimensionless geometrical and topological parameters of the porous medium affecting the flow (e.g. porosity, genus, coordination number, normalized chamber and throat size distributions, chamber-to-throat size correlation factors, etc.). Note that in equation (1)  $S^w$  is *not* considered to be an *independent* variable; actually,  $S^w$  is one of the dependable variables in the system of DeProF equations.

### Basics of the DeProF Model

In the general case of SS2fFPM of Figure 1(a), the physical system of the porous medium, oil and water is characterized by the values of the physicochemical parameters, namely  $\tilde{\gamma}_{\text{ow}}, \tilde{\mu}_o, \tilde{\mu}_w, \theta_A^0, \theta_R^0, \mathbf{x}_{\text{pm}}$ . Oil and water are continuously supplied along the macroscopic flow direction,  $\tilde{z}$ , with constant flowrates  $\tilde{q}^o$  and  $\tilde{q}^w$ , so that the operational (dimensionless) parameters  $\text{Ca}$  &  $r$  have constant values.

In the CPF region the oil retains its connectivity and flows with virtually one-phase flow. The porous medium volume fraction occupied by the connected oil is denoted by  $\beta$ . The DOF regime is defined as the region composed of the rest of the unit cells, so the DOF volume fraction equals  $(1-\beta)$ . Water is the wetting phase and always retains its connectivity. DOF implicitly represents the connected-water pathway flow. A microscopic scale representation (a snapshot) of a typical DOF region is shown in Figure 1(b). An oil ganglion having a typical “cruising” configuration [5,6,8] is shown at the center. All the cells that accommodate parts of this (or any other) oil ganglion are called *ganglion cells* and are demarcated with a thick dashed line. The rest of the cells in the DOF region are cells containing water and oil drops. These cells comprise the regions of the GD and DTF domains respectively.

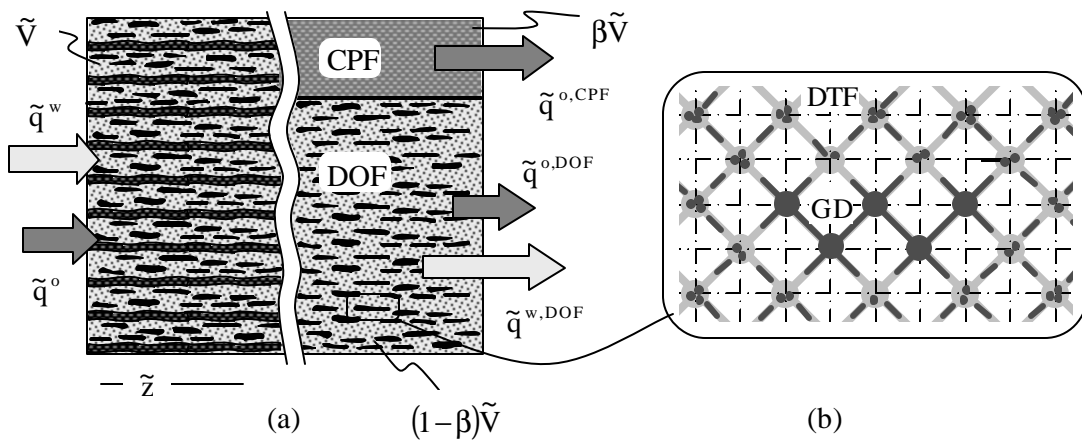


**Figure 1** (a) “Actual” flow and its theoretical decomposition into prototype flows: CPF & DOF. (b) A microscopic scale representation (snapshot) of a DOF region. An oil ganglion of size class 5 is shown. For simpler representation, all cells are shown identical and the lattice constant is shown expanded. The dashed line separates the GD cells domain and the DTF cells domain. In reality chambers and throats have prescribed size distributions.

The fraction of all the ganglion cells over all the DOF region cells is denoted by  $\omega$ , and is called the GD domain fraction. The DTF domain fraction in the DOF region equals  $(1-\omega)$ .  $S^w$ ,  $\beta$  and  $\omega$  are called *flow arrangement variables* (FAP) because they give a coarse indication of the prevailing flow pattern. One of the objectives of DeProF is to determine the values of  $S^w$ ,  $\beta$  and  $\omega$  that conform with the externally imposed conditions. The overall flowrates are partitioned in the prototype flows;  $\tilde{q}^{o,CPF}$ ,  $\tilde{q}^{o,DOF}$  are the mean oil flowrates in CPF, and DOF and  $\tilde{q}^{w,DOF}$  the mean water flowrate in DOF. The following physical quantities are also assigned to the prototype flows: the reduced oil mean superficial velocity in CPF, defined by  $U^{o,CPF} = \tilde{q}^{o,CPF} / \tilde{q}^o$  and the reduced oil and water mean

superficial velocities defined by  $U^{m,DOF} = \tilde{q}^{m,DOF} / \tilde{q}^m$ , where  $m=o,w$ . It is assumed that oil ganglia and drops move with equal superficial velocities.

The flow analysis is carried out at two length scales, a macroscopic scale ( $10^{12}$  pores, or more) and a microscopic scale, and produces a system of equations that includes macroscopic water and oil mass balances, flow arrangement relations at the macroscopic scale, equations expressing the consistency between the microscopic and macroscopic scale representations in the DOF region and an equation that is obtained by applying effective medium theory to the “equivalent one -phase flow” in the DOF (GD&DTF) region -implicitly representing the transfer function for this region [5,6]. The system is closed by imposing an appropriate type of distribution function for the ganglion volumes, which is dictated by the physics of ganglion dynamics.

For any given set of  $(Ca, r; \kappa, \theta_A^0, \theta_R^0, \mathbf{x}_{pm})$  values all physically admissible combinations of the values of  $(S^w, \beta, ?)$ , are determined. By assuming equal probability for each admissible solution and averaging over their domain, a unique solution for the macroscopic flow is obtained, in the form of equation (1).

Macroscopic interstitial physical quantities, such as the magnitude of the domain of physically admissible solutions, the interfacial area per unit volume, the mechanical power dissipation per unit volume, the degree of disconnectedness of the non-wetting phase, and the flow parameter domain over which two-phase flow is sustained, the reduced superficial velocity of o/w interfaces, and the fraction of interface transport through DTF, can be computed in a straightforward manner.

We will use the predictive capability of the DeProF model to investigate whether optimum operating conditions with respect to oil flowrate exist in steady-state two-phase flow in pore networks. By ‘*optimum operating conditions*’ we mean those values of  $Ca$  and  $r$  (the operating parameters of the system) for which the ratio of oil flow rate over the mechanical power dissipation takes one (or many) locally maximum values. To this end, we introduce a new dependent variable, namely, the energy utilization factor,  $f_{EU}$ . This is a macroscopic variable defined as the ratio of the reduced o/w flow rate ratio over the reduced rate of mechanical energy dissipation,  $f_{EU} = r/W$ ; it is a measure of the efficacy of the physical process under consideration in terms of oil flowrate per unit energy cost.  $W$  is the reduced rate of mechanical energy dissipation in steady-state two-phase flow in pore networks; it is calculated [5] as the weighted sum of the reduced rates of mechanical energy dissipation in each prototype flow:

$$W \equiv \tilde{W} \tilde{k}_{\tilde{u}_w} (\tilde{\gamma}_{ow} Ca)^{-2} = \beta r U^{o,CPF} + [(1-\beta)r U^{o,DOF} + 1] x \quad (2)$$

where,  $x = (-\partial \tilde{p} / \partial \tilde{z}) \tilde{k} (\tilde{\gamma}_{ow} Ca)^{-1}$  is the reduced macroscopic pressure gradient,  $\tilde{k}$  is the permeability. The mechanical power that is externally supplied to the system equals the rate of mechanical energy dissipation. Mechanical energy dissipation is caused interstitially: (a) by bulk viscous stresses in combination with the local rates of deformation, and (b) by

capillary pressure in combination with the velocities of moving menisci and contact angle hysteresis effects. Clearly, the relative magnitude of the two contributions depends among other factors on the degree of disconnection of oil (the non-wetting phase).

### Simulations of Steady-State Two-Phase Flow in Pore Networks

A number of simulations of steady-state fully developed two-phase flows in two-dimensional (2D) and three-dimensional (3D) pore networks of the chamber-and-throat type were carried out using the DeProF model. Three typical systems were examined, with system parameter values  $\tilde{\gamma}_{ow} = 25 \times 10^{-3} \text{ N/m}$ ,  $\theta_w^0 = 45^\circ$ ,  $\theta_R^0 = 39^\circ$ , and  $\beta = 0.66, 1.45$  and  $3.35$ . The simulations performed covered a rectangular domain in  $(Ca, \log r)$ , from  $(Ca, \log r) = (10^7, -1)$  to  $(Ca, \log r) = (10^5, 2)$ . The domain was covered in successive steps of  $Ca = 0.5 \times 10^{-6}$  (20 steps in the  $Ca$  range) and of  $\log r = 0.2$  (16 steps in the  $\log r$  range).

### Pore Network Geometry and Topology

The simulations were carried out for 2D and 3D pore networks of the chamber-and-throat type. The two lattices used in the simulations are, square in the 2D case, cubic in the 3D case (identical to those described in [8]). A schematic representation of the two types of network is shown in Figure 2. Chambers and throats are sited at the nodes and branches of the networks. The network lattice constant is the same in both networks. There are 5 classes of chamber sizes and 5 classes of throat sizes in both networks and we assume that there is no correlation between the classes of chambers and throats. Both pore networks are isotropic. In all simulations, the pressure gradient (or macroscopic flow since both networks are isotropic) is parallel (a) to the square diagonal of the 2D network (45deg to the principal axes), and (b) to the cubic diagonal of the 3D network.

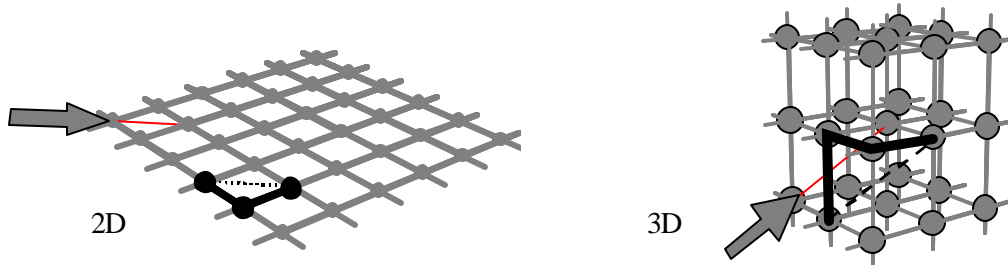


*Figure 2* The two dimensional (left) and three dimensional (right) pore networks used in the simulations. In both cases the lattice constant is shown expanded for better visualization. The thick arrow indicates the direction of the macroscopic flow relative to the principal axes of the network.

In the 2D network all chambers are right short circular cylinders. The throats are cylinders with elliptical cross-sections. The geometry of the 2D pore network is identical to the geometry of the glass model pore network used in the experiments of Avraam & Payatakes [1,2], and in the DeProF model simulations of Valavanides & Payatakes [5,6,8].

The volume porosity of the 2D pore network is  $e=0.0306$  while its absolute permeability is  $\tilde{k} = 8.890 \mu\text{m}^2$ . In the 3D network the chambers are spheres and the throats are right cylinders. The hydraulic conductances of the 3D network throats are equal to those of the 2D network. The volume porosity of the 3D pore network is  $e=0.0464$  while its absolute

permeability is  $\tilde{k}=8.965 \mu\text{m}^2$ . The absolute permeabilities of the two networks are practically equal.

A feature which is important to the modelling of two-phase flow in pore networks is the tortuosity of a typical ganglion,  $\tau^G$ . Moving ganglia have a tendency to become aligned as far as possible with the macroscopic flow direction, acquiring the so-called ‘cruising shape’ [6,9,10,11,12]. We assume that all ganglia have a zigzag spine that is aligned with the macroscopic pressure gradient. The tortuosity of a ganglion is equal to the average ratio of the ganglion actual length over the length projected in the macroscopic flow direction [6,8]. In Figure 2, using black bold lines, the typical cruising shapes of a ganglion of size 3 in a 2D network and of a ganglion of size 4 in a 3D network are depicted. The respective length projections on the direction of the macroscopic flow are depicted with the dashed black lines. For the 2D network,  $\chi_{2D}^G = \sqrt{2}$ , while for the 3D network,  $\chi_{3D}^G = \sin^{-1} \arctan(\sqrt{2}/2) \approx 1.732$ .

## Results

The results of the simulations are presented in Figures 3 to 6. Due to space limitations results are mainly presented from simulations pertaining to o/w systems with  $\kappa=1.45$  and for the 3D network; when results for other cases are presented we make special reference. All simulations were carried out over the  $(Ca, r)$  domain for which two-phase flow is sustainable. In Figure 3 the DeProF model predictions for the reduced rate of mechanical energy dissipation,  $W$ , and the reduced macroscopic pressure gradient,  $x$ , are presented.

In Figure 4 the DeProF predictions are presented for the flow arrangement variables ( $S^w$ ,  $\beta$ , and  $\omega$ ) and for the reduced superficial velocity of o/w interfaces,  $U^{ow,DOF}$ , the coefficient of oil fragmentation,  $f_{OF}$ , and the fraction of interface transport through DTF,  $\xi^{ow,D}$  defined in [8].

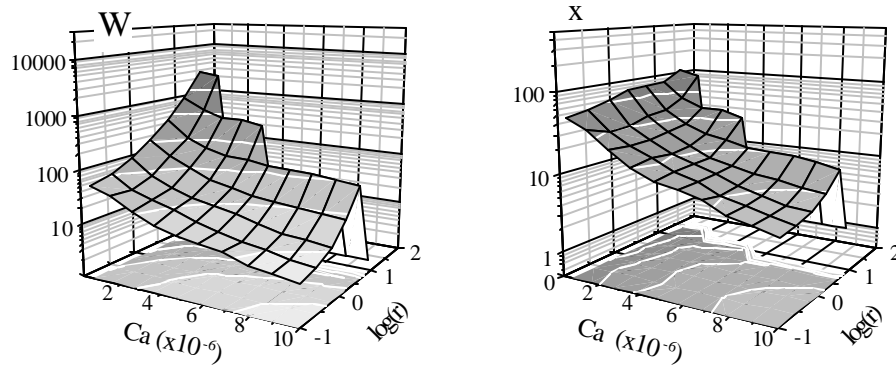


**Figure 3** Reduced mechanical power dissipation of the total flow,  $W$ , and reduced pressure gradient,  $x$ , as a function of  $Ca$  and  $r$ . The diagrams pertain to 3D pore network simulations for an o/w system with viscosity ratio  $\kappa = 1.45$ .

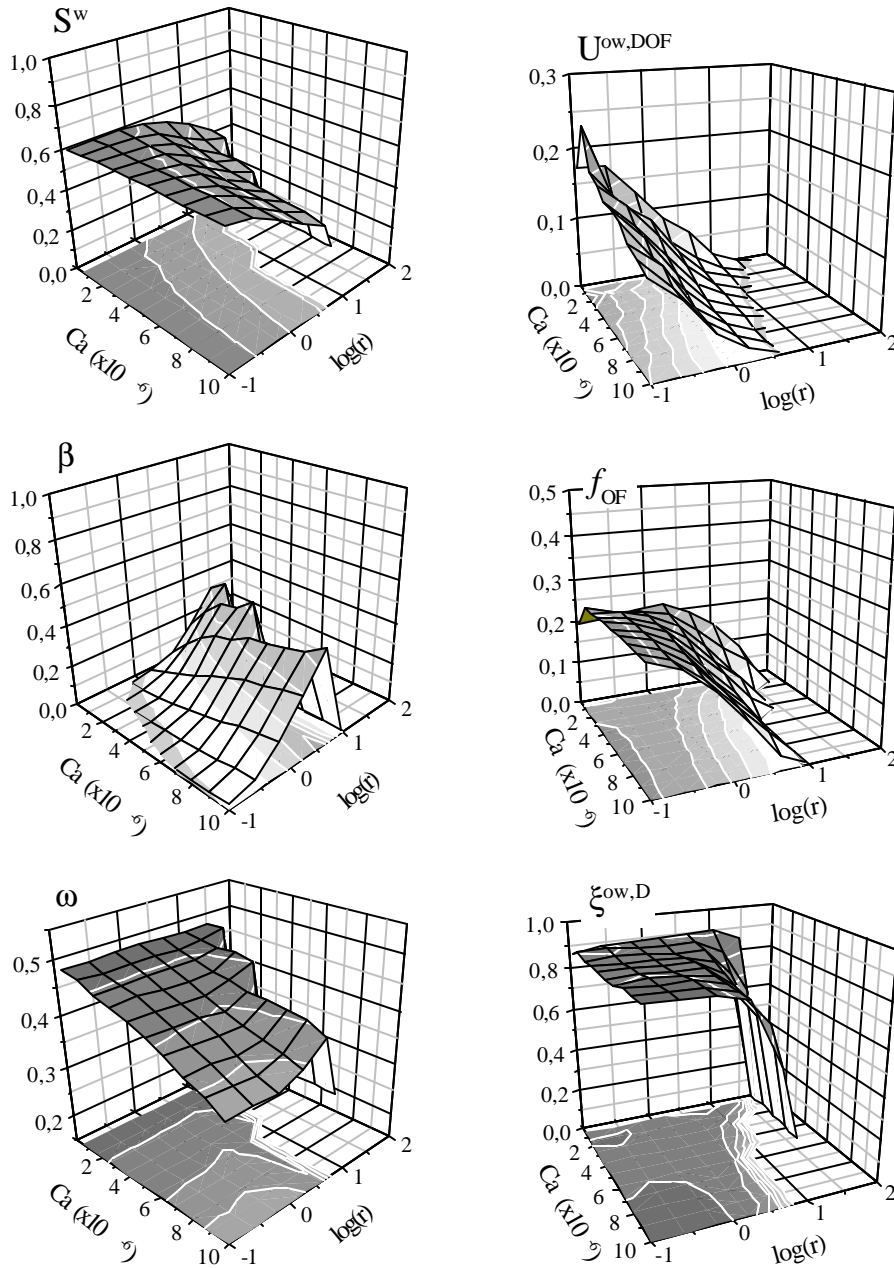


*Figure 4* Flow arrangement variables  $S^w$ ,  $\beta$  and  $\omega$ , reduced superficial velocity of o/w interfaces,  $U^{ow,DOF}$ , coefficient of oil fragmentation,  $f_{OF}$ , and fraction of interface transport through DTF,  $\xi^{ow,D}$ , as a function of  $Ca$  and  $r$ . The diagrams pertain to 3D pore network simulations for an o/w system with viscosity ratio  $\kappa = 1.45$ .



The results for the energy utilization factor  $f_{EU} (=r/W)$  are represented by the hump-shaped surfaces in the diagrams of Figures 5 & 6. It appears that for every system, there exists a continuous line in the  $(Ca, r)$  domain for which the energy utilization factor takes locally maximum values. This line is the projection of the  $r/W$  surface ridge on the  $(Ca, r)$  plane. Thus we conclude that for every constant value of  $Ca$ , there exists a particular value of the flowrate ratio,  $r^*(Ca)$ , for which the energy utilization factor becomes maximum. In other words, oil flowrate per kW of power externally supplied to the system becomes maximum.

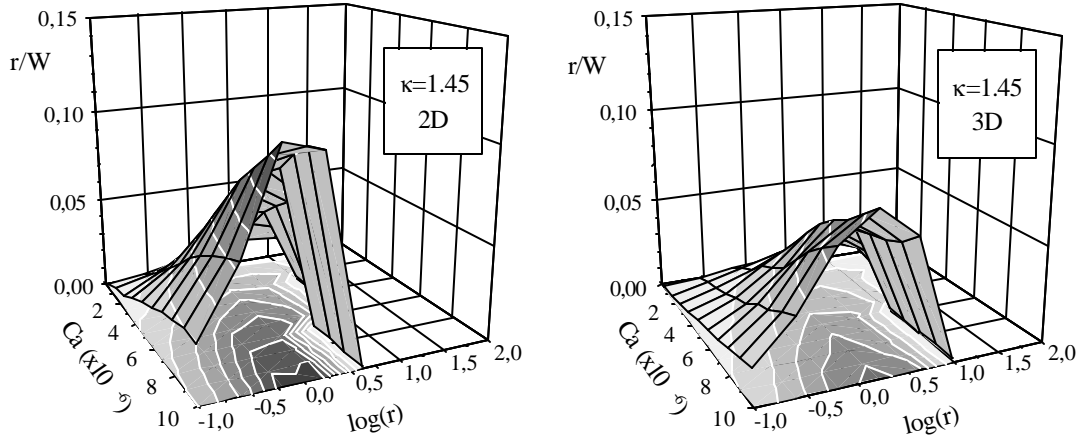


**Figure 5** Effect of pore network dimensionality on the energy utilization factor ( $f_{EU}=r/W$ ) as a function of  $Ca$  and  $r$ . The viscosity ratio of the o/w system is set at  $\kappa = 1.45$ .

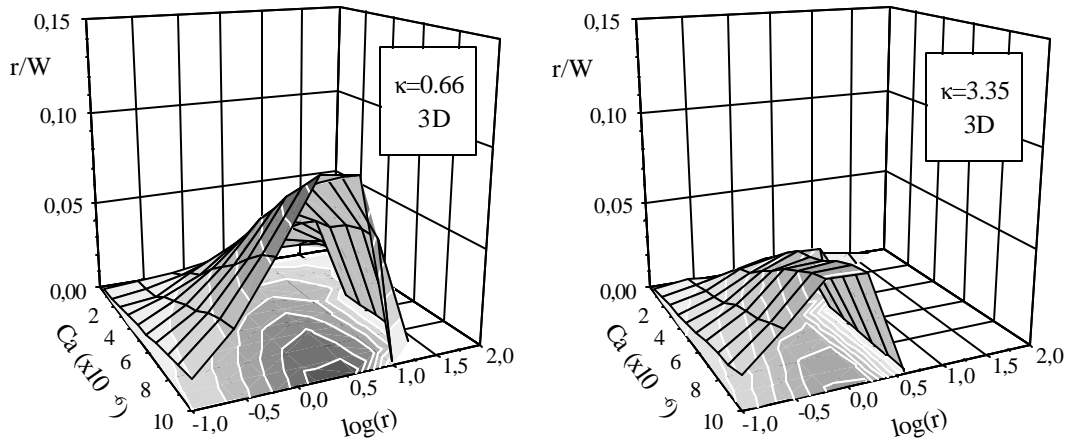


**Figure 6** Effect of the viscosity ratio,  $\kappa$ , on the energy utilization factor ( $f_{EU}=r/W$ ) as a function of  $Ca$  and  $r$  in the 3D network.

In the following we will try to explain this behavior using phenomenological arguments. First we discuss the effect of  $Ca$  on  $f_{EU}$  with constant  $r$ . As  $Ca$  increases ( $r=\text{const.}$ ),  $W$  decreases (see Figure 3), therefore,  $r/W$  increases. We recall here that  $W$  is the reduced mechanical power dissipation with respect to the mechanical power dissipation of the equivalent one-phase flow [ $\tilde{W}^{1\phi} = Ca^2 \tilde{\gamma}_{ow}^2 / (\tilde{\mu}_w \tilde{k})$ ]. As  $Ca$  increases, the flow of oil tends to shift towards the CPF regime (the CPF regime expands and occupies larger parts of the pore network on the expense of ganglia; in Figure 4,  $S^w$  remains practically constant,  $\beta$  increases and  $\omega$  decreases). Consequently, bulk viscous stresses begin to dominate capillary effects and therefore, the rate of mechanical energy dissipation is mainly caused by viscous stresses. Comparing Figures 5 & 6 one can also observe that the increase in  $r/W$  becomes more pronounced as  $\kappa$  decreases. The reason for this is the following. The value of interfacial tension,  $\tilde{\gamma}_{ow}$ , is practically the same in all three systems considered here, and therefore the relative magnitude of capillary effects, compared to bulk viscous stresses, increases so long as  $\kappa$  decreases. Since, for the case of low  $\kappa$  examined here, capillary effects predominate over bulk phase viscosity, the system becomes more sensitive to an increase in  $Ca$  (i.e. a reduction of the capillary effects) and  $r/W$  increases sharply. We have not carried out any numerical simulations for  $Ca$  values above  $10^{-5}$ , but we expect that the value of  $r/W$  as  $Ca$  increases further, with constant  $r$ , tends asymptotically to a limiting value.

The effect of  $r$  on  $f_{EU}$  ( $=r/W$ ) with constant  $Ca$  is more complicated. For every constant value of  $Ca$ , a unique local maximum for  $f_{EU}$  is observed as  $r$  takes values in the domain of sustainable two-phase flows. For relatively small values of  $r$  ( $-1 < \log r < -0.25$ ), an increase in  $r$  causes an increase in  $f_{EU}$ . The reason is not quite obvious. In order to increase  $r$  -with constant  $Ca$ - the flow rate of oil should be increased; the system seeks a new flow arrangement by (a) expanding the connected oil pathways ( $\beta$  increases, see Figure 4), (b) slightly reducing the oil fragmentation with the formation of small ganglia at the expense of oil droplets ( $f_{OF}$  and  $U^{w,DOF}$  decrease, see Figure 4). The consequence is that the contribution of capillary effects to the rate of mechanical energy dissipation becomes significantly larger. Trading droplets for ganglia reduces the number of menisci but small ganglia are harder to mobilize than droplets [8]. Therefore, when  $r$  increases -at small  $r$ - the value of  $W$  also increases but with a small to moderate rate (Figure 3). Both  $r$  and  $W$  increase, but  $W$  increases slower than  $r$  and so  $f_{EU}$  increases. The increase in  $f_{EU}$  is more pronounced for  $\kappa=0.66$  than it is for  $\kappa=3.35$  because, as discussed in the previous paragraph, for  $\kappa=0.66$  the system is more sensitive to capillary effects. With further increase in  $r$  ( $-0.25 < \log r$ ), the fraction of porous medium occupied by connected oil,  $\beta$ , further increases (Figure 4) and, simultaneously, the disconnected oil -in the form of oil droplets- tends (better “is forced”) to organize in larger oil entities, such as larger ganglia ( $\omega$  increases and  $f_{OF}$ , the fraction of oil fragmentation [8], decreases sharply). For reasons already explained in [8], ganglia in pore networks of the type considered here are more difficult to mobilize and to keep moving, compared to oil droplets. (This effect would be further enhanced if we consider a lubricated film around the droplets.) Therefore, the capillary effects become even more pronounced and  $W$  increases at a rate now higher than

before. The combined result is that  $f_{EU}$  decreases, and the efficacy of the process is progressively reduced.

The same behavior was observed for systems with  $\kappa$  equal to 0.66 and 3.35 in both 2D and 3D networks. For every fixed value in  $Ca$  there exists a unique value in  $r$ ,  $r^*(Ca)$ , for which  $f_{EU}$  ( $=r/W$ ) attains a local maximum value. Since  $r^*$  is a continuous function of  $Ca$ , a continuous line  $r = r^*(Ca; \kappa, \theta_A^0, \theta_R^0, \mathbf{x}_{pm})$  exists that extends over the domain of  $(Ca, r)$  values for which two-phase flow is sustainable.

## CONCLUSIONS

The predictive capability of the *DeProF* model was used to investigate the existence of optimum operating conditions in steady-state two-phase flow in pore networks. By introducing a new macroscopic physical quantity, the energy utilization coefficient,  $f_{EU}$ , defined as  $f_{EU}=r/W$ , we have assessed the efficacy of the process with respect to the maximization of the oil transport per kW of mechanical power supplied to the system. Our calculations show that for every fixed value in  $Ca$  there exists a unique value in  $r$ ,  $r^*(Ca)$ , for which  $f_{EU}$  ( $=r/W$ ) attains a local maximum value. Thus, there exists a continuous line  $r = r^*(Ca; \kappa, \theta_A^0, \theta_R^0, \mathbf{x}_{pm})$ , in the domain of  $(Ca, r)$  values for which two-phase flow is sustainable, along which the operation of the system is at its most efficient in terms of oil flowrate per unit energy cost.

It is worth noting that tackling the problem of the existence of ‘optimum’ conditions in an overall (“holistic”) sense reveals no clear and consistent answer. Here the predictive capabilities of the *DeProF* model are extremely useful; a detailed /analytic examination of the flow using a few specially selected macroscopic interstitial physical quantities, such as the interfacial area per unit volume, the mechanical power dissipation per unit volume, the degree of disconnection of the non-wetting phase, and the rate of o/w interface transfer [8], gives one the capability to characterize the physical system in a straightforward manner and come up with some basic conclusions.

The existence of ‘optimum conditions’ for oil transport in steady-state two-phase flow in pore networks is a consequence of the remarkable internal adaptability of the flow to externally imposed flow conditions  $(Ca, r)$  and its inherent characteristic in trading-off between connected pathway flow, ganglion dynamics and drop traffic flow and self adjusting the connected versus disconnected moving-oil balance.

Two-dimensional pore networks have been used in the past to study SS2f flow in porous media on a laboratory scale. There has always been a great deal of skepticism on whether the observed behavior of two-phase flow in pore networks is representative of two-phase flows in real porous media. The results of the present work show the potential of using pore network hierarchical models, such as *DeProF*, to elucidate the physics of two-phase

flow in real porous media in a self consistent way. In future works the effects of pore-size correlation and network heterogeneities should be investigated along the same lines.

## REFERENCES

1. Avraam, D.G., & Payatakes, A.C.: "Flow Regimes and Relative Permeabilities during Steady-State Two-Phase Flow in Porous Media", *J. Fluid Mech.*, (1995) **293**, 207-236.
2. Avraam, D.G., & Payatakes, A.C.: "Flow Mechanisms, Relative Permeabilities and Coupling Effects in Steady-State Two-Phase Flow in Porous Media. Case of Strong Wettability", *Industrial & Engineering Chemistry Research*, (1999) **38**, 778-786.
3. Payatakes A.C., & Valavanides, M.S.: "True-to-Mechanism Macroscopic Theory of Steady-State Two-Phase Flow in Porous Media", Proceedings, in V.N. Burganos et al. (Editors): "*Computational Methods in Water Resources XII*", Vol. 2, *Comput. Mechanics Publications*, Boston, USA, (1998), 3-10.
4. Valavanides, M.S. & Payatakes, A.C.: "Prediction of the relative permeabilities for steady-state two-phase flow in porous media, using a mechanistic-thermodynamic model", (1998), *ECMOR VI 6<sup>th</sup> European Conference on the Mathematics of Oil Recovery; Proc. Intern. symp.*, Peebles near Edinburgh, Scotland, September 8-11.
5. Valavanides, M.S. & Payatakes A.C., &.: "A True-to-Mechanism Model of Steady-State Fully Developed Two-Phase Flow in Porous Media, Including the Contribution of the Motion of Ganglia and Droplets", *Computational Methods in Water Resources XIII*, Bentley et al. (eds), Balkema, Rotterdam, ISBN 90 5809 123 6, (2000), 239-243.
6. Valavanides, M.S., & Payatakes, A.C.: "True-to-Mechanism Model of Steady-State Two-Phase Flow in Porous Media, using Decomposition into Prototype Flows", *Advances in Water Resources*, (2001) **24**, 385-407.
7. Kirkpatrick, S.: "Percolation and Conduction", *Reviews of Modern Physics*, (1973) **45**(4), 574-588.
8. Valavanides, M.S., & Payatakes, A.C.: "Effects of Pore Network Characteristics on Steady-State Two-Phase Flow Based on a True-to-Mechanism Model (DeProF)", (2002), *SPE 78516, 10<sup>th</sup> ADIPEC Abu Dhabi International Petroleum Exhibition & Conference*, Abu Dhabi, United Arab Emirates, October 13-16, pp.379-387
9. Constantinides, G.N. & Payatakes, A.C.: "Network Simulation of Steady-State Two-Phase Flow in Consolidated Porous Media", *AICHE J.*, (1996) **42**(2), 369-382.
10. Melrose, J.C. & Bradner, C.F.: "Role of Capillary Forces in Determining Microscopic Displacement Efficiency for Oil Recovery by Water Flooding", *J. Can. Petr. Tech.*, (1974) **13**, 54-62.
11. Payatakes A.C.: "Dynamics of Oil Ganglia During Immiscible Displacement in Water-Wet Porous Media", *Ann. Rev. Fluid Mech.*, (1982) **14**, 365-393.
12. Valavanides, M. S., Constantinides, G. N., and Payatakes, A. C.: "Simulation of the Motion of Oil Ganglia in Consolidated Porous Media. Crowding Effects", (1996), *ECMOR V, Proc. 5<sup>th</sup> European Conference on the Mathematics of Oil Recovery*, Leoben, Austria, 355-364.